Edge Computing-Based Cyber-Physical Interdependent Power Restoration of Active Distribution Networks

Hao Yu, *Senior Member, IEEE*, Zhicheng Zhang, Peng Li*, *Senior Member, IEEE*, Haoran Ji, *Senior Member, IEEE*, Guanyu Song, *Senior Member, IEEE*, Jiancheng Yu, Jinli Zhao, *Member, IEEE*, and Jianzhong Wu, *Fellow, IEEE*

***Abstract*—The digitalization of distribution networks intensifies the coupling between cyber and physical networks. Edge computing devices offer significant flexibility for organizing distributed energy resources and enabling multi-area coordinated control, demonstrating considerable potential to enhance the power restoration capability of active distribution networks. This paper proposes a power restoration method based on edge computing technology, which accounts for the interdependencies between cyber and physical systems during the restoration process. For the cyber system, a self-organization method for edge computing devices is proposed to establish a dual-layer emergency communication network, supporting strategy generation for power restoration. For the physical system, an ADMM-based solving method is developed to achieve rapid solution of the restoration problem in a distributed manner by pre-fixing binary variables. Case studies are conducted on the IEEE 123-node test system and the Taiwan 94-node test system, highlighting the advantages of the proposed method in terms of restoration speed and effectiveness.**

***Index Terms*—active distribution network; edge computing; cyber-physical system; power restoration**

NOMENCLATURE

Sets and Indices:

Ω_z	Set of nodes belong to zone z
$\Omega_{i,\mathrm{c}}$	Set of child nodes of node i
$\Omega_{i,\mathrm{p}}$	Set of parent nodes of node i
Ω_s	Set of nodes connected to switches
N_z/N_z^*	Set of zones and set of zones without main sources
$\Omega_{i,\mathrm{s}}$	Set of nodes connected to node i by switches
Ω_{e}	Set of available EC devices
D	Set of available terminal devices

Variables:

α_{ij}	Status of the switch between nodes i, where $\alpha_{ij,n}$=0 if the switch is open; otherwise, $\alpha_{ij,n}$=1 if the switch is closed
β_{ij}/β_{ji}	The power flow direction of the switches between nodes i and j
b_i	Control state of the terminal device i
cs_i	Controlled state of terminal device in node i, where cs_i=1 represents node i is under control
$\gamma_{n,l,i}$	Signal-to-noise ratio of the communication link l between EC device i to the terminal device n
$\gamma_{j,i}$	Signal-to-noise ratio of the between EC device i to j
$g_{n,l,i}$	Gain in the communication link l between EC device i to the terminal device n
$g_{j,i}$	Gain in the communication link between EC device i to EC device j
μ_i^j	Control state of the terminal device, where μ_i^j =1 represents terminal device j is controlled by EC device i
n_i^{blk}	The number of bus blocks in EC device i's control domain
P_{ij}/Q_{ij}	Active power/reactive power flowing from node i to node j [MW, Mvar]
$P_i^{\mathrm{G}}/Q_i^{\mathrm{G}}$	Active/ reactive generation at node i [MW, Mvar]
$P_{n,l,i}$	The communication power of the l-th subcarrier from EC device i to the terminal device n.
$P_{j,i}$	The communication power of link from EC device i to j
$R_{n,i}/R_{j,i}$	Communication rate between EC device i and terminal device n/ EC device j [bit/s]
s_i	Load shedding at node i[pu]
$\tau_{n,i}/\tau_{j,i}$	Time delay between EC device i and terminal device n/ EC device j
$\theta_{n,l,i}$	$\theta_{n,l}$ =1 represents sub-carrier l is allocated to the communication link between EC device i to the terminal device n
V_i	Square voltage magnitude at node i [kV^2]

Parameters:

a	The pathloss exponent
α_1/α_2	The coefficients for computational burden assessment
$\overline{d}$	Maximum radius of the EC device's control domain
$d_{n,i}/d_{j,i}$	The distance between EC device i to the terminal device n/ EC device j
e_i	Value coefficient of load at node i [pu]
ε	ADMM algorithm convergence tolerance
h	The loss factor combining total fading effects
H	The node number of the multi-hop path $\mathcal{H}$
L_i	Maximum number of subcarriers for EC devices i
N_0	The noise power
$n_{\mathrm{d}}/n_{\mathrm{e}}$	The number of terminal devices/ EC devices
n_i^{sw}	The number of switches connected to node i
$\overline{O_i^{\mathrm{cp}}}$	Maximum computational burden of the EC device i
P_0	Inherent power consumption of EC devices
$\overline{P_i^{\mathrm{cm}}}$	Maximum communication burden of the EC device i
$P_i^{\mathrm{l}}/Q_i^{\mathrm{l}}$	Active/ reactive load demand at node i [MW, Mvar]
$\overline{P_i^{\mathrm{G}}}/\overline{Q_i^{\mathrm{G}}}$	Maximum active/ reactive power generated at node i [MW, Mvar]
r_{ij}/x_{ij}	Resistance/ reactance of branch ij
$\underline{R}$	The minimum communication rate required
$\underline{\gamma}$	The minimum signal-to-noise ratio required
$\overline{S}_{ij}$	The maximum capacity of line ij [MVA]

This work was supported by the National Natural Science Foundation of China (U24B6010, 52307132) and Tianjin Natural Science Foundation Project (24JCYBJC01250).

Hao Yu, Zhicheng Zhang, Peng Li, Haoran Ji, Guanyu Song and Jinli Zhao, are with the State Key Laboratory of Smart Power Distribution Equipment and System, Tianjin University, Tianjin 300072, China (e-mail: lip@tju.edu.cn).

Jiancheng Yu is with the State Grid Tianjin Electric Power Research Institute, Tianjin 300072, China.

Jianzhong Wu is with the Institute of Energy, School of Engineering, Cardiff University, CF24 3AA Cardiff, U.K.

$S_{n,i}$	The size of the data packets transmitted between EC device n and the terminal device i [bit]
$\bar{\tau}$	The max allowable communication rate
$\overline{V}/\underline{V}$	Max/ min voltage square magnitude [kV^2]
v_i	The importance of the terminal device i
w	The bandwidth of the subcarrier

I. INTRODUCTION

Distribution networks, as the final stage of electrical power delivery, play a crucial role in ensuring a continuous and reliable power supply to end users [1]. The integration of distributed generators (DGs) and advanced automation equipment facilitates the transition towards active distribution networks (ANDs) [2], enabling the autonomous coordination of power restoration resources for self-healing during emergencies [3]. However, natural disasters such as typhoons, floods, and earthquakes, as well as human-made events, can cause simultaneous damage to communication and electrical equipment [4]. Although such extreme events are infrequent, they can lead to large-scale blackouts resulting in significant economic loss [5]. Enhancing the capability for rapid power restoration in scenarios where both cyber and physical systems are compromised has become a critical and widely discussed topic in distribution networks.

Power restoration methods for distribution networks have been extensively studied, which can be primarily classified into centralized and distributed methods. Centralized methods require the distribution management system (DMS) to monitor and control all the equipment. These methods generally require favorable communication conditions, which are challenging to satisfy under extreme events. In contrast, distributed methods only require local communications among neighboring controllers [6]. In emergency scenarios, the communication links required for distributed methods are more adaptive. Additionally, distributed methods decompose the overall power restoration problem into multiple sub-problems, alleviating the computational burden.

Distributed methods can be primarily categorized into heuristic methods [7], mathematical optimization methods [8], and learning-driven methods [9]. Among these, mathematical optimization methods are capable of ensuring the optimality and feasibility of the power restoration strategy. Thus, they are widely applied in practice. The alternating direction method of multipliers (ADMM) algorithm is the most widely used distributed mathematical optimization algorithm. However, the conventional ADMM algorithm cannot address the power restoration problem due to the presence of binary variables for switch actions. To address this issue, a projection function-based ADMM (P-ADMM) was proposed for the distributed solution of the power restoration problem, wherein binary variables were derived through a projection function [6][10]. However, the incorporation of the projection function leads to an escalation in the number of iterations. By introducing proximal operators in the ADMM algorithm, binary variables are guided to converge more efficiently toward Boolean values [11]. This modification reduces the time consumption required to solve the power restoration problem, thereby enhancing its potential for practical application.

The edge computing (EC) devices enable the deployment of various distributed power restoration algorithms, which offers significant flexibility and can remain feasible under extreme fault conditions that would render centralized methods inoperative. The EC devices are able to facilitate the rapid self-organization of available resources, establish effective emergency communication networks, and formulate optimized restoration strategies for the physical network [12]. In this context, the physical system supply restoration becomes increasingly reliant on the cyber systems [13]. Most power restoration methods optimistically assume that the cyber system remains unscathed during power failures. However, communication facilities such as base stations may be damaged after the fault, rendering the original communication network inoperative. The assumption may be over-optimistic, as it overlooks the reality that extreme events can inflict damage not only on the physical system but also on the cyber system [14].

Efforts have been made to address the cyber-physical system (CPS) interdependent power restoration problems. The majority of these methods leverage a diverse range of external resources to establish emergency communication networks, facilitating the power restoration process. For example, literature [15] proposed an optimal scheduling method for crews to repair damaged components in both cyber and physical systems. In [16], a wireless emergency communication network was established after the disaster by dispatching emergency communication vehicles. Literature [17] established a wireless communication network with high topology flexibility using the unmanned aerial vehicle (UAV) small cell. Literature [18] deployed a drone-enabled mesh emergency communication network to restore coverage in the affected area when the base station is inoperative. A reconnection method for offline network devices based on 5G technology was proposed in [19].

Emergency communication networks can also be established by creating multi-hop connections between controllers and terminal devices within the ADN. In [20], an optimal scheduling approach was proposed for the routing path from the central controller to every router, minimizing the cascading effects from the initial fault. Literature [21] established an ad hoc wireless device-to-device emergency communication network after the disaster to support physical system restoration. A centralized approach was used to establish distributed controller-to-controller emergency communication networks by developing anticipated accident sets in advance in [22]. Emergency networks and EC devices are vulnerable to cyber threats in real-world scenarios. To enhance resilience and ensure data integrity, approaches such as encrypted data transmission [23], integrity verification [24], and attack detection [25] can be employed. These approaches can be integrated into the EC-based emergency networks to enhance cyber resilience and to satisfy zero-trust requirements.

EC devices can be used to form emergency communication networks in a distributed manner, providing advantages such as rapid deployment, high survivability, reliability, and wide coverage. However, current CPS interdependent power restoration methods still rely on the functioning of the control center and critical communication equipment, subject to the inherent limitations of centralized methods. There remains a gap in methods for power restoration based on EC devices. Additionally, the consideration of CPS interdependency is still insufficient. At the cyber layer, existing methods primarily

focus on factors such as network delay and power consumption, neglecting the effects of the cyber system in generating and implementing the restoration strategy. At the physical layer, the complicated restoration strategy generation methods usually demand a considerable amount of computation, which is challenging for the constrained battery capacity and computational capability of EC devices during power failures.

The CPS interdependent restoration problem of ADN is highly complex, making it difficult to address in a holistic manner. Therefore, this study adopts a sequential approach, in which the cyber system is restored first, followed by the physical system, with their interdependencies considered throughout the process. As illustrated in Fig. 1, a significant portion of loads is interrupted following the fault. During the cyber restoration phase, a dual-layer multi-hop emergency communication network is established, restoring control over terminal devices and increasing the power restoration potential. Once the cyber system is restored, physical restoration is carried out using an ADMM-based strategy with the support of the emergency communication network, converting this potential into actual load recovery.

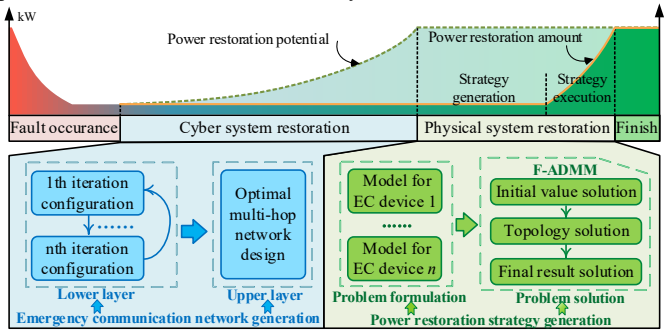

Fig.1. Process of cyber-physical interdependent power restoration.

The specific contributions of this study are summarized as follows:

1) A distributed power restoration framework is established for ADNs, considering the interdependencies between the cyber system and physical system during the power restoration process. The model is developed to describe the impact of physical network resource organization schemes on the computational and communication burdens of EC devices.

2) A method for rapidly generating dual-layer emergency communication networks following faults is proposed. The lower-layer cyber system is established using a search-based approach, which determines the control domain of each EC device. The upper-layer cyber system is established utilizing the shortest-path approach, which establishes the communication link among all EC devices.

3) An ADMM-based solving method, termed F-ADMM, is developed for solving the physical system restoration strategy. This method effectively reduces the number of iterations by separately solving and fixing the binary variables in advance, making it well-suited for distributed power restoration based on the EC platform, where the EC devices and emergency cyber system may have limited survival time.

II. CPS Restoration Problem Formulation

In this study, EC devices are utilized to generate power restoration strategy and issue commands to the terminal controllers. The terminal controllers are deployed at each node within the physical network to manage the loads, DGs, and switches connected to that node. During a fault event, both the EC devices in the cyber system and the electrical equipment in the physical system may sustain damage. These damaged devices are incapable of participating in the CPS interdependent restoration. The CPS interdependent restoration problem is formulated based on the devices that remain functional.

During cyber system restoration, the EC devices autonomously reorganize to establish an emergency dual-layer cyber system, as depicted in Fig. 2. The upper-layer cyber system utilizes multi-hop mechanisms to enable communication among EC devices and facilitate their cooperation. The EC devices generate power restoration strategy by executing distributed algorithm via the upper-layer network. The lower-layer cyber system adopts point-to-point communication to connect the EC devices with their associated terminal controllers. Once the power restoration strategy is determined, the EC devices disseminate it to the terminal devices via the lower-layer network. Both layers are assumed to operate based on wireless communication for greater flexibility.

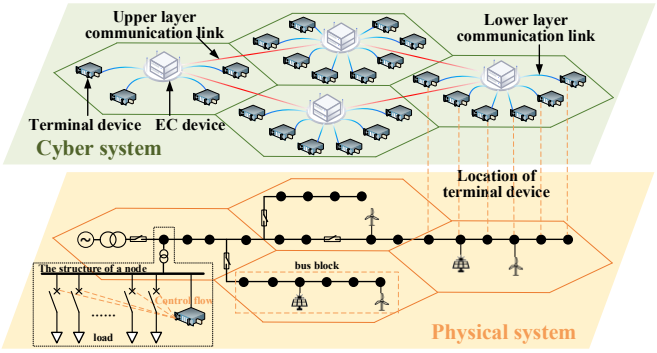

Fig.2. Schematic of the CPS interdependency in ADN.

The formation of the dual-layer emergency communication network is modeled as the cyber system restoration problem, while the supply restoration of the physical network is modeled as the physical system restoration (PSR) model. The interaction between the two models is expressed as follows: The PSR model for each EC device is formulated based on its control domain determined by the cyber system restoration. Correspondingly, in the cyber system restoration (CSR) model, the computational difficulty of the PSR model for each EC device is assessed. These two models are detailed below.

A. Physical System Restoration (PSR) Model

Constrained by its limited computational capacity, the EC device faces challenges in solving large-scale problems. To reduce computational complexity, the power restoration problem of ADN is modeled as a mixed-integer linear programming (MILP) problem. For each EC device's domain, the power restoration model is expressed as follows.

Objective: The objective function of PSR model is to maximize the restoration amount of critical loads, as expressed in (1). Critical loads refer to the loads whose interruption would lead to significant social and economic disruptions, such as hospitals, emergency services, and key industrial facilities. The criticality of the load at each node is quantified using a value

coefficient that reflects the socioeconomic impact of its outage. It is assumed that these value coefficients are predetermined by the power company prior to the restoration process.

$$f_{\mathrm{p}} = \min \sum_{i\in\Omega_z} -P_i^{\mathrm{l}} e_i s_i \tag{1}$$

Constraints: The constraints of the PRS model include power flow constraints, operational constraints, and topology constraints.

1) Power flow constraint: The linearized Distflow model is employed to describe the power flow constraints, as outlined in (2)-(5). Eqs. (6)-(7) ensure no power flows through the branch with an open switch. M represents a large constant. Eq. (8) describes the impact of the cyber system on the physical system, specifying that only nodes controlled by an EC device are eligible for load restoration.

$$\sum_{h\in\Omega_{i,\mathrm{p}}} P_{hi} + P_i^{\mathrm{G}} = P_i^{\mathrm{l}}(1-s_i) + \sum_{j\in\Omega_{i,\mathrm{c}}} P_{ij} \tag{2}$$

$$\sum_{h\in\Omega_{i,\mathrm{p}}} Q_{hi} + Q_i^{\mathrm{G}} = Q_i^{\mathrm{l}}(1-s_i) + \sum_{j\in\Omega_{i,\mathrm{c}}} Q_{ij} \tag{3}$$

$$V_i - V_j = 2\left(P_{ij}r_{ij} + Q_{ij}x_{ij}\right), j \in \Omega_{i,\mathrm{c}} \tag{4}$$

$$-\overline{V}\left(1-\alpha_{ij}\right) \le V_i - V_j \le \overline{V}\left(1-\alpha_{ij}\right), j \in \Omega_{i,\mathrm{c}} \cap \Omega_{\mathrm{s}} \tag{5}$$

$$-M\alpha_{ij} \le P_{ij} \le M\alpha_{ij}, j \in \Omega_{i,\mathrm{c}} \cap \Omega_{\mathrm{s}} \tag{6}$$

$$-M\alpha_{ij} \le Q_{ij} \le M\alpha_{ij}, j \in \Omega_{i,\mathrm{c}} \cap \Omega_{\mathrm{s}} \tag{7}$$

$$0 \le s_i \le cs_i \tag{8}$$

The linearized DistFlow model neglects the network loss term, usually leading to underestimation of node voltages compared with their actual values [26]. In power restoration scenarios, where node voltages commonly fall below the lower limits due to limited power capacity, the strategy obtained from the linearized model becomes more conservative. Therefore, the linearized model demonstrates good feasibility for power restoration problems.

2) Operational constraints: Eqs. (9)-(10) denote constraints on the voltage magnitudes and branch capacity, respectively. Eqs. (11)-(12) constrain the magnitudes of active and reactive power generated at each node.

$$\underline{V} \le V_i \le \overline{V} \tag{9}$$

$$0 \le P_{ij}^2 + Q_{ij}^2 \le \overline{S}_{ij} \tag{10}$$

$$0 \le P_i^{\mathrm{G}} \le \overline{P_i^{\mathrm{G}}} \tag{11}$$

$$0 \le Q_i^{\mathrm{G}} \le \overline{Q_i^{\mathrm{G}}} \tag{12}$$

3) Topology constraint: Given the widespread adoption of the "closed-loop design, open-loop operation" paradigm in modern distribution networks, the network topology after restoration is required to be radial. Eqs. (13)-(16) denote the topological constraints for a bus block, which are used to ensure the radial configuration of ADN [27]. A bus block is defined as a group of nodes interconnected by non-switched branches. Eq. (13) ensures that the power flow through any closed switch must be unidirectional. Eq. (14) constrains power flow in bus blocks with a main source to outward direction only. Eq. (15) requires that in bus blocks without a main source, at most one closed switch allows inflow, while all others permit only outward flow.

$$\beta_{ij} + \beta_{ji} = \alpha_{ij}, j \in \Omega_{i,\mathrm{c}} \cap \Omega_{\mathrm{s}} \tag{13}$$

$$\beta_{ji} = 0, j \in \Omega_{i,\mathrm{c}} \cap \Omega_{\mathrm{s}}, z \in N_z/N_z^* \tag{14}$$

$$\sum_{i\in\Omega_z}\left(\sum_{h\in\Omega_{i,\mathrm{p}}\cap\Omega_{\mathrm{s}}} \beta_{hi} + \sum_{j\in\Omega_{i,\mathrm{c}}\cap\Omega_{\mathrm{s}}} \beta_{ji}\right) = 1, z \in N_z^* \tag{15}$$

$$\beta_{ij}, \beta_{ji} \in [0,1] \tag{16}$$

The domain of each EC device may encompass nodes from different bus blocks. Thus, the topological constraints for each zone encompass the topological constraints of all bus blocks whose nodes fall within the zone's boundary.

The compact form of the PSR model for each EC device can be expressed as follows:

$$\begin{aligned} &\min f_{\mathrm{p}} \\ &\text{s.t.}(2)-(16) \end{aligned} \tag{17}$$

B. Cyber System Restoration (CSR) Model

The CSR model entails organizing the controllable EC devices and terminal devices to establish an emergency communication network after the fault. The surviving edge computing devices are assumed to be equipped with backup batteries, enabling them to self-organize. The cyber system restoration is carried out in two stages. First, the lower-layer cyber system is formed by determining the control domain of each EC device. Then, the upper-layer cyber system is established by creating communication paths between each EC device based on the lower-layer cyber system.

The lower-layer cyber system determines the organization of power restoration resources. The PSR model for each EC device is formulated based on this organization. Thus, the primary task for cyber system restoration is to establish an effective lower-layer cyber system. The reconfiguration of the cyber system is achieved through the distributed interaction of EC devices. For each EC device, the CSR model is formulated as follows:

Objective: Cyber systems should possess high survivability and extensive coverage. Survivability can be assessed by the power consumption, while coverage can be evaluated by the number of controlled terminal devices. Thus, the goal of the CSR model is to optimize the emergency communication network by maximizing the integration of critical devices while concurrently reducing the communication burden P_i^{cm} and computational burden O_i^{cp}. The objective function for EC device i is expressed as:

$$f_{\mathrm{c}} = \min -c_{\mathrm{d}} \sum_{j=1}^{n_{\mathrm{d}}} v_j b_j + c_{\mathrm{cm}} P_i^{\mathrm{cm}} + c_{\mathrm{cp}} O_i^{\mathrm{cp}} \tag{18}$$

where c_{d}, c_{cm}, c_{cp} denote the weight coefficients of the controlled devices value, the communication burden and the computational burden, respectively. They are set based on experience and can be adjusted according to the actual needs of power restoration.

The importance of a terminal device v_j is determined by its affiliated loads, DGs, and switches, which is calculated as:

$$v_j = c_{\mathrm{l}} e_j P_j^{\mathrm{l}} + c_{\mathrm{G}} P_j^{\mathrm{G}} + c_{\mathrm{sw}} n_j^{\mathrm{sw}} \tag{19}$$

where c_{l}, c_{G}, c_{sw} denote the weight coefficients of each term.

The communication burden is the power consumption requirement for establishing communication link with all terminal devices within its domain [29], as expressed by:

$$P_i^{\mathrm{cm}} = \sum_{n=1}^{n_{\mathrm{d}}} \sum_{l=1}^{L_i} P_{n,l,i} \tag{20}$$

The computational burden is the difficulty of solving the PSR

model for EC devices. Since the problem is formulated as a MILP, its computational difficulty grows exponentially with the number of nodes in worst-case scenarios [28]. The number of bus blocks also affects complexity, as they introduce additional topological constraints and binary variables. Thus, the computational burden of each EC device is defined as:

$$O_i^{\mathrm{cp}} = e^{\alpha_1 \sum_{j=1}^{n_{\mathrm{d}}} \mu_i^j + \alpha_2 n_{\mathrm{blk}}} \tag{21}$$

where α_1, α_2 denote the weight coefficients of node number and bus block number. Note that the assessment using (21) reflects a worst-case complexity analysis. In practice, solvers may use optimization techniques to reduce computational demands, so the burden estimated by (21) could be conservative.

Constraints: The constraints of the CSR model include communication rate constraints, subcarrier allocation constraints, communication quality constraints, and EC device operational constraints.

1) Communication quality constraints: These constraints ensure reliable information transmission within the cyber system. The instantaneous communication rate, signal-to-noise ratio, and time delay are used as quality indicators, calculated by (22)-(25) [29]. To meet reliability requirements, these indicators must comply with ADN communication quality standards specified in (26)-(28) [30].

$$R_{n,i} = \sum_{l=1}^{L} \theta_{n,l,i} w \log_2(1 + \gamma_{n,l,i}) \tag{22}$$

$$\gamma_{n,l,i} = P_{n,l,i} g_{n,l,i} / N_0 \tag{23}$$

$$g_{n,l,i} = h d_{n,i}^{-a} \tag{24}$$

$$\tau_{n,i} = S_{n,i} / R_{n,i} \tag{25}$$

$$R_{n,i} \geq \underline{R} \tag{26}$$

$$\gamma_{n,l,i} \geq \theta_{n,l,i} \underline{\gamma} \tag{27}$$

$$\tau_{n,i} \leq \bar{\tau} \tag{28}$$

2) Subcarrier allocation constraints: The EC devices establish connections with terminal devices by allocating subcarriers, which should meet the following constraints. Eq. (29) denotes the exclusivity constraint of the subcarriers, i.e., only one terminal device can be connected to each subcarrier [22]. Eq. (30) guarantees that if the communication link is absent, no power is allocated on that link. Eq. (31) denotes there is at least one communication link between the EC device and the terminal device it controls. Eq. (32) is used to calculate the controlled state of terminal device j.

$$\sum_{n=1}^{n_{\mathrm{d}}} \sum_{i=1}^{n_{\mathrm{e}}} \theta_{n,l,i} \leq 1, \forall l \in L_i \tag{29}$$

$$0 \leq P_{n,l,i} \leq M \theta_{n,l,i} \tag{30}$$

$$\mu_i^j = \begin{cases} 0, \sum_{l=1}^{L_i} \theta_{n,l,i} = 0 \\ 1, \sum_{l=1}^{L_i} \theta_{n,l,i} \geq 0 \end{cases} \tag{31}$$

$$cs_j = \sum_{i=1}^{n_{\mathrm{e}}} \mu_i^j \tag{32}$$

3) Device constraints: The cyber system should meet the device constraints of the EC devices. Eq. (33) denotes the maximum control radius for each EC device. Eqs. (34)-(35) denote the computational power limit and power consumption limit for the EC device, respectively.

$$d_{n,i} \leq \overline{d} \tag{33}$$

$$O_i^{\mathrm{cp}} \leq \overline{O_i^{\mathrm{cp}}} \tag{34}$$

$$P_i^{\mathrm{cm}} + P_0 \leq \overline{P_i^{\mathrm{cm}}} \tag{35}$$

The compact form of the CSR model for each EC device can be expressed as follows:

$$\begin{aligned} &\min f_{\mathrm{c}} \\ &\text{s.t.} (22) - (35) \end{aligned} \tag{36}$$

In this section, the restoration models for the physical system and cyber system are established. The preceding section will describe how to generate solutions for the CPS interdependent restoration.

III. Solving Method for Cyber System Restoration

To achieve rapid restoration of the cyber system, a two-stage solution generation method is developed in this study. In the first stage, the lower-level cyber system is established using a sequential decision-making approach based on greedy searching. In the second stage, the upper-layer cyber system is established by employing the shortest-path approach.

A. Solution of Lower-Layer Communication Network

The holistic lower-layer cyber system restoration scheme is composed of the scheme of EC devices. For each EC device, the lower-layer cyber system scheme consists of two main components: 1) The controlled devices set, which specifies the terminal devices that are controlled by this EC device. 2) The communication resource allocation scheme, which is designed to establish efficient communication paths with the controlled terminal devices.

Solving problem (36) is challenging due to the presence of the logarithmic function and binary variables. However, once the terminal devices controlled by the EC device i are determined, the communication resource allocation problem for EC device i can be expressed as (37). By stipulating that communication between EC device i and terminal device n occurs via a pre-assigned subcarrier l, i.e., $\theta_{n,l,i}$ in (37) is given, problem (37) is further simplified to a small-scale convex problem.

$$\begin{aligned} &\min P_{n,l,i} \\ &\text{s.t.} (22) - (30) \end{aligned} \tag{37}$$

Thus, this paper proposes a search-based method to address the lower-layer cyber system restoration problem. Each EC device explores possible controlled devices sets that satisfy the constraints, and solves the problem (37) for each set. By solving multiple small-scale problems rather than tackling the complex CSR model directly, this approach enables the rapid generation of cyber system restoration solutions. The architecture of the lower-layer cyber system generation process is shown in Fig.3.

As depicted in Fig.3, the lower-layer network is generated through iterations of a two-layer nested loop. In the inner loop, the EC device conducts a series of sequential decision-making based on the predefined order. Specifically, from EC 1 to EC n, each EC device takes turns making decisions and repeats this cycle until the stopping condition is met. Whenever the inner loop iteration is completed, a new configuration strategy for the lower-layer cyber system is devised. Then, in the outer loop, the EC devices adjust their parameters based on the newly formed configuration strategy to facilitate the equalization of computational burden among EC devices.

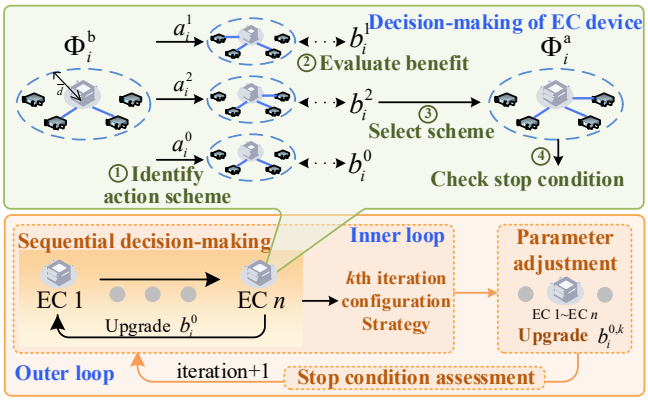

Fig.3. Architecture of the lower-layer cyber system generation.

1) Decision-making of EC devices

The decision-making of each EC device is based on greedy searching. Initially, the EC device enumerates all possible action schemes at the current moment. Let A_i represent the set of all possible action schemes of EC device i, and Φ_i represent the set of terminal devices controlled by EC device i. The elements in A_i include: i) a_i^n (n $\neq$ 0): incorporate terminal device n into Φ_i. According to (33), terminal device n is the device whose distance from EC device i is less than $\overline{d}$. ii) a_i^0: not incorporate any device and maintain current Φ_i.

Subsequently, the EC device assesses the benefit of each action scheme. The benefit of the action scheme a_i^n, denoted by b_i^n, is calculated as follows:

For a_i^n(n$\neq$0), b_i^n represents the increment in the objective function for CSR model after executing a_i^n. It can be calculated as follows: Let Φ_i^{b} and Φ_i^{a} represent the Φ_i before and after executing a_i^n, respectively.

For the specified Φ_i^{a}, n_{blk} and μ_i^j is given, the communication resource allocation scheme can be obtained by solving (37). Then, the computational burden for the EC device is calculated by (21), and the communication burden of the EC device i is obtained by (20). Thus, the objective function value of the CSR model can be obtained by (18).

It should be noted that not all possible action schemes are feasible due to constraints (34) and (35). For the feasible action schemes, b_i^n is calculated by (38). Otherwise, b_i^n is set to -M, ensuring the corresponding action scheme will not be selected.

$$b_i^n = f_{\mathrm{c}}^{\mathrm{a}} - f_{\mathrm{c}}^{\mathrm{b}} \tag{38}$$

where $f_{\mathrm{c}}^{\mathrm{b}}$ represents the value of (18) with Φ_i^{b}, $f_{\mathrm{c}}^{\mathrm{a}}$ represents the value of (18) with Φ_i^{a}.

For a_i^0, the benefits b_i^0 for each EC device are different and are predetermined in the parameter adjustment process. It denotes the threshold value. If all b_i^n(n$\neq$0) are lower than the b_i^0, the EC device executes a_i^0.

In this way, the benefits of all action schemes can be derived. Then, the EC device selects the scheme with the greatest benefit and executes it.

Once the scheme is executed by the EC device, the stop condition check is performed. The stopping condition is satisfied when, for all EC devices, the set A_i only contains 1) a_i^0 and 2) a_i^n with b_i^n being -M.

2) Parameter Adjustment of EC Devices

b_i^0 is upgraded during the lower-layer cyber system restoration process, intending to equalize the computational burden among all EC devices. This is important for improving power restoration efficiency because the distributed solving process of the PSR model must be synchronized among all EC devices. The adjustment of b_i^0 is divided into two parts.

i) When the inner loop is completed and a new configuration strategy of the lower-layer cyber system is generated, the initial value of b_i^0 for the next inner loop is upgraded by (39).

$$b_i^{0,k} = b_i^{0,k-1} + \rho(O_i^{\mathrm{cp}} - \textstyle\sum_{i=1}^{n_{\mathrm{e}}} O_i^{\mathrm{cp}} / n_{\mathrm{e}}) \tag{39}$$

where $b_i^{0,k}$ is the value for b_i^0 in the kth iteration, $b_i^{0,k-1}$ is the value for b_i^0 in the k-1th iteration, ρ is a constant.

In this way, an EC device with a high computational burden in the current strategy increases its b_i^0. This adjustment makes this EC device more inclined to choose the action a_i^0, thereby reducing its computational burden in the next iteration.

ii) Within each inner loop, once EC 1 to EC n have made their decisions, b_i^0 is upgraded as follows: If all EC devices choose a_0, the r_0 value is incremented according to (40). This minimizes the possibility that all EC devices will still choose a_0 in the next round of decision-making. Otherwise, the r_0 value remains unchanged.

$$b_i^{0\prime} = b_i^0 + r_c \tag{40}$$

where $b_i^{0\prime}$ represents the updated b_i^0, r_c represents a constant.

3) Stop condition for the outer loop

After parameter adjustment, the stop condition for the outer loop is assessed. If the variance in the computational burden among all EC devices falls below a predefined threshold or the number of iterations reaches the set maximum number, the iterative process is halted. And the strategy generated in this iteration is adopted as the final lower-layer cyber system configuration strategy.

B. Solution of Upper-Layer Communication Network

After the lower-layer cyber system is restored, the domain of each EC device is determined. If there is a physical network connection between the domains of two distinct EC devices, an upper-layer communication link should be established between these two EC devices. This upper-layer communication link is achieved through the multi-hop mechanism, i.e., information is forwarded through multiple intermediate EC devices during transmission from the source EC device to the target EC device.

The multi-hop path determination problem for each EC device is formulated as a shortest-path problem, where each device is modeled as a node and each single-hop link as an edge. The objective of the upper-layer cyber system restoration is to ensure the reliability and survivability of the multi-hop network. Accordingly, the weight of each single-hop link is defined by two factors: 1) the power consumption $P_{k,k+1}$, which should be minimized to conserve battery resources; and 2) the packet loss rate $p_{k,k+1}$, which may arise from environmental disturbances and should be minimized to enhance reliability. The weight of each link can be expressed as $\mathrm{c}_{\mathrm{pwr}} p_{k,k+1} + \mathrm{c}_{\mathrm{loss}} p_{k,k+1}$, and the total weight of a multi-hop path $\mathcal{H}$={(1, 2)…(k, k+1)…(H-1, H)} can be written as (41).

$$w_{\mathcal{H}} = \mathrm{c}_{\mathrm{pwr}} \textstyle\sum_{k=1}^{H-1} P_{k,k+1} + \mathrm{c}_{\mathrm{loss}} (1 - \prod_{k=1}^{H-1} (1 - p_{k,k+1})) \tag{41}$$

In (41), the first term denotes the total communication power consumption for establishing the multi-hop path, while the

second term reflects its total packet loss rate. Owing to the dynamic nature of communication environments, packet loss rates are usually modeled by probability distribution functions $\boldsymbol{F}_{k,k+1}$ [31], which transforms the problem into a stochastic shortest-path problem. The optimal path is thus identified as the one with the minimal expected weight [32]. As links between EC devices are established independently, packet loss rate distributions are also assumed to be independent, and the total weight of the multi-hop path can be expressed as:

$$E(w_{\mathcal{H}}) = \mathrm{c}_{\mathrm{pwr}} \sum_{k=1}^{H-1} P_{k,k+1} + \mathrm{c}_{\mathrm{loss}}\left(1 - \prod_{k=1}^{H-1}(1 - \mathrm{E}(\boldsymbol{F}_{k,k+1}))\right) \quad (42)$$

where $\mathrm{E}(\boldsymbol{F}_{k,k+1})$ denotes the expectation value of $\boldsymbol{F}_{k,k+1}$.

To ensure the communication quality of the upper-layer network, each multi-hop path must satisfy constraints (43)-(50). Eqs. (43)-(48) specify that each single-hop link is assigned a single subcarrier and must satisfy the quality constraints. The total delay of a multi-hop path is modeled as the sum of individual link delays, as given in (49). Eq. (50) enforces that the overall delay meets the communication quality standard.

$$R_{k,k+1} = \sum_{l=1}^{L} w \log_2(1 + \gamma_{k,k+1}) \quad (43)$$

$$\gamma_{k,k+1} = P_{k,k+1} g_{k,k+1} / N_0 \quad (44)$$

$$g_{k,k+1} = h d_{k,k+1}^{-a} \quad (45)$$

$$\tau_{k,k+1} = S_{k,k+1} / R_{k,k+1} \quad (46)$$

$$R_{k,k+1} \geq \underline{R} \quad (47)$$

$$\gamma_{k,k+1} \geq \underline{\gamma} \quad (48)$$

$$\tau_{\mathrm{total}} = \sum_{k=1}^{H-1} \tau_{k,k+1} \quad (49)$$

$$\tau_{\mathrm{total}} \leq \bar{\tau} \quad (50)$$

Thus, the total weight of the multi-hop path $\mathcal{H}$ can be obtained by solving for the minimum $E(w_{\mathcal{H}})$ subject to (43)-(50), expressed as:

$$\begin{aligned} &\min E(w_{\mathcal{H}}) \\ &\text{s.t.} (43)-(50) \end{aligned} \quad (51)$$

Using the expected weight of a multi-hop path, the upper-layer communication restoration is formulated as a shortest-path problem. The modified Floyd-Warshall algorithm is employed to generate candidate paths under different allowable hop counts, using approximate weights obtained by summing the constituent single-hop link weights. The accurate total weights of these candidates are then evaluated using (51), and the multi-hop path with the smallest total weight is selected as optimal. The detailed procedure is attached in the Appendix.

The cyber system restoration method presented above can be fully implemented on the EC platform, realizing the self-organization of distributed resources and EC devices. Although this approach may not achieve full optimality, it avoids directly solving the non-convex CSR model and generates a feasible strategy online, providing a concise and efficient solution for power restoration.

IV. Solving Method for Physical System Restoration

The PSR model is a MILP problem and can be solved by the modified ADMM algorithm. However, existing ADMM-based methods may face the issue of a high iteration number, because the binary variables do not easily converge. In this study, considering that the binary variables α_{ji} represent the switch states, they can be decoupled from the holistic restoration model to relieve the solving difficulty. Thus, the Fixation-ADMM (F-ADMM) solving method is developed, which first solves the binary variables separately, fixes their values, and subsequently solves the remaining continuous variables.

A. Variable Division

To ensure the consistency of solutions in different zones, the variables within each EC device's domain are extended and categorized into distinct classes:

To ensure solution consistency across different zones, the variables within each EC device's domain are extended and classified into distinct categories. For simplicity, the nodes in an EC device's domain are first divided into internal nodes and boundary nodes.

1) The variables $\mathbf{X}$ to be solved in the PSR model (17), which consists of the internal-node variables $\mathbf{X}_{\mathrm{in}}$ and the boundary-node variables $\mathbf{X}_{\mathrm{b}}$. Moreover, the boundary variables $\mathbf{X}_{\mathrm{b}}$ are further separated into binary variables $\boldsymbol{X}_{\mathrm{b}}^{\mathrm{bin}}$ and continuous variables $\boldsymbol{X}_{\mathrm{b}}^{\mathrm{cont}}$, expressed as:

$$\mathbf{X}_{\mathrm{b}} = \{P_{ij}, Q_{ij}, P_i^{\mathrm{G}}, Q_i^{\mathrm{G}}, V_i, \beta_{ij}, \beta_{ji}, \alpha_{ij}\} \quad (52)$$

$$\boldsymbol{X}_{\mathrm{b}}^{\mathrm{bin}} = \{\alpha_{ij}\} \quad (53)$$

$$\boldsymbol{X}_{\mathrm{b}}^{\mathrm{cont}} = \{P_{ij}, Q_{ij}, P_i^{\mathrm{G}}, Q_i^{\mathrm{G}}, V_i, \beta_{ij}, \beta_{ji}\} \quad (54)$$

2) Consensus variables $\mathbf{Y}$ of the ADMM algorithm:

$$\mathbf{Y} = \{\tilde{P}_{ij}, \tilde{Q}_{ij}, \tilde{P}_i^{\mathrm{G}}, \tilde{Q}_i^{\mathrm{G}}, \tilde{V}_{ij}, \tilde{\beta}_{ij}, \tilde{\beta}_{ji}, \tilde{\alpha}_{ij}\} \quad (55)$$

where the tilde denotes the consensus copies of the original variables maintained by the coordinator in ADMM.

3) Dual variables $\boldsymbol{\Lambda}$ of the ADMM algorithm:

$$\boldsymbol{\Lambda} = \{\kappa_{ij}, \chi_{ij}, \kappa_i, \vartheta_i, \vartheta_i, \pi_{ij}, \gamma_{ji}, \mu_{ij}\} \quad (56)$$

where the elements of $\boldsymbol{\Lambda}$ denotes the dual variables of the original variables in $\mathbf{X}_{\mathrm{b}}$.

B. Process of F-ADMM

Compared to the conventional ADMM algorithm that solves the entire problem at once, this method solves the power restoration problem through three stages: initial value solution, topology solution, and result solution. The process of F-ADMM solving method is shown in Fig.4, which converts the original complex non-convex problem into a small-scale non-convex problem and two convex problems.

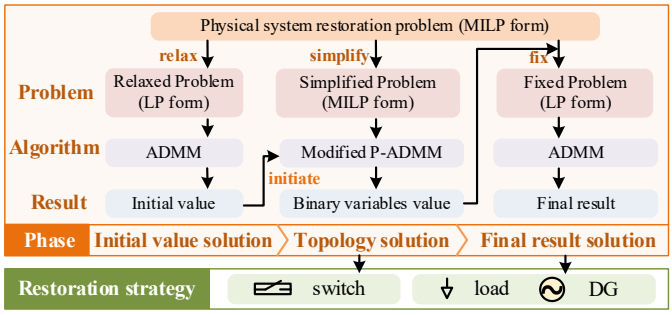

Fig.4. Process of the proposed F-ADMM solving method.

1) Initial value solution

In this phase, binary variables $\boldsymbol{X}_{\mathrm{b}}^{\mathrm{bin}}$ within the original problem (17) are treated as continuous variables, and the objective function is transformed into (57). Subsequently, the ADMM algorithm [33] is applied to solve the relaxed problem, deriving the initial solution. The steps for the k-th iteration in

the ADMM algorithm are outlined as follows:

(i) Solve (58) to get the value of $\mathbf{X}_\mathrm{b}$ in the k-th iteration.

$$f^\mathrm{I} = f_\mathrm{p} + \|\mathbf{X}_\mathrm{b} - \mathbf{Y}^{k-1} + \mathbf{\Lambda}^{k-1}\|^2 - \|\mathbf{\Lambda}^{k-1}\|^2 \quad (57)$$

$$\begin{matrix}\mathrm{argmin}_{\mathbf{X}}\, f^\mathrm{I} \\ \mathrm{s.t.}(2)-(16)\end{matrix} \quad (58)$$

where the superscript 'k-1' indicates the value of that variable obtained in the k-1th iteration.

(ii) Solve the unconstrained quadratic programming problem (59) to get the value of $\mathbf{Y}$ in the k-th iteration.

$$\mathrm{argmin}_{\mathbf{Y}}\, f^\mathrm{II} \quad (59)$$

$$f^\mathrm{II} = f_\mathrm{p} + \left\|\mathbf{X}_\mathrm{b}^k - \mathbf{Y} + \mathbf{\Lambda}^{k-1}\right\|^2 - \|\mathbf{\Lambda}^{k-1}\|^2 \quad (60)$$

(iii) Update the dual variables by (61).

$$\mathbf{\Lambda}^k = \mathbf{\Lambda}^{k-1} + (\mathbf{X}_\mathrm{b}^k - \mathbf{Y}^k) \quad (61)$$

(iv) Check the convergence of the ADMM algorithm by (62). If convergence has been achieved, stop the iteration and obtain $\boldsymbol{X}_\mathrm{b}^{\mathrm{bin},k}$ as the initial value for the topology solution phase.

$$\left\|\mathbf{X}_\mathrm{b}^k - \mathbf{Y}^k\right\|_\infty \le \varepsilon \quad (62)$$

2) Topology solution

In this phase, the binary variables of the PSR model are separated, deriving a simplified problem with the objective function of (1) and the constraints of (13)-(16). Accordingly, the boundary variables $\mathbf{X}_\mathrm{b}$, consensus variables $\mathbf{Y}$, and dual variables $\mathbf{\Lambda}$ are respectively transformed as:

$$\mathbf{X}_\mathrm{b} = \{\beta_{ij}, \beta_{ji}, \alpha_{ij}\} \quad (63)$$

$$\mathbf{Y} = \{\tilde{\beta}_{ij}, \tilde{\beta}_{ji}, \tilde{\alpha}_{ij}\} \quad (64)$$

$$\mathbf{\Lambda} = \{\pi_{ij}, \gamma_{ji}, \mu_{ij}\} \quad (65)$$

The topology solution is derived by a P-ADMM-based iteration process. An additional term is incorporated into the objective function of the P-ADMM [6] to accelerate the convergence of $\mathbf{X}_\mathrm{b}$ towards binary values. The steps for the k-th iteration are outlined as follows:

(i) Relax α_{ij} in the topology configuration problem to continuous variables. Solve (66) to get the value of $\mathbf{X}_\mathrm{b}$ in the current iteration. f^I is expressed as (57).

$$\begin{matrix}\mathrm{argmin}_{\mathbf{X}}\, f^\mathrm{I} \\ \mathrm{s.t.}(13)-(16)\end{matrix} \quad (66)$$

(ii) Obtain the value of $\mathbf{Y}_\mathrm{proj}$ by (67). Solve the unconstrained quadratic programming problem (68) to get the value of $\mathbf{Y}$ in the current iteration.

$$\mathbf{Y}_\mathrm{proj} = \prod_\mathrm{proj}(\mathbf{X}^k) \quad (67)$$

$$\mathrm{argmin}_{\mathbf{Y}}\, f^\mathrm{tp} \quad (68)$$

$$f^\mathrm{tp} = \frac{1}{2t}(\|\mathbf{X}^k - \mathbf{Y} + \mathbf{\Lambda}^{k-1}\|^2 + \|\mathbf{\Lambda}^{k-1}\|^2) + \frac{1}{2}(\left\|\mathbf{Y} - \mathbf{Y}_\mathrm{proj}\right\|^2) \quad (69)$$

where $\prod_\mathrm{proj}$ denotes the projection function, which rounds $\mathbf{Y}$ to the nearest binary value. t denotes the incentive parameter. A large value of t compels the variable $\mathbf{Y}$ to gravitate towards binary values.

(iii) Update the dual variables by (61).

(iv) Update the incentive parameter t by (70). As the number of iterations increases, the value of t keeps increasing, which helps to accelerate the convergence.

$$t' = t + \omega_1(1/r_\mathrm{p}^k + 1/r_\mathrm{d}^k) + \omega_2 \quad (70)$$

$$r_\mathrm{p}^k = \left\|\mathbf{X}_\mathrm{b}^k - \mathbf{Y}^k\right\|^2 \quad (71)$$

$$r_\mathrm{d}^k = \|\mathbf{Y}^k - \mathbf{Y}^{k-1}\|^2 \quad (72)$$

where r_p^k and r_d^k are the primal and dual residuals. ω_1 and ω_2 denote constants.

(iv) Check the convergence by (62). If convergence has been achieved, stop the iteration and obtain $\mathbf{X}_\mathrm{b}^k$ as the topology configuration solution for PSR model.

3) Final result solution

In this phase, the binary variables $\mathbf{X}_\mathrm{b}^\mathrm{bin}$ of the original problem (17) are fixed based on the result of $\mathbf{X}_\mathrm{b}$ obtained from the topology solution phase, forming a LP model. Subsequently, the ADMM algorithm in the initial solution phase is applied to solve the fixed model, deriving the final restoration strategy.

The overall F-ADMM solving steps are summarized in Algorithm 1.

Algorithm 1: F-ADMM solving method

Input: The PSR model (17)
Output: Power restoration strategy
Initialization: iteration index k = 0; r_p^0=r_d^0=1;
Formulate the problem for the initial value solution
while Eq (62) is met **do**
    Solve (58) to get $\mathbf{X}_\mathrm{b}^k$
    Solve (59) to get $\mathbf{Y}^k$
    Update the dual variables by (61), $k = k$+1
end
*After this loop, the initial solution for $\mathbf{X}_\mathrm{b}$ is obtained
Formulate the problem for the topology solution
while Eq (62) is met **do**
    Solve (66) of to get $\mathbf{X}_\mathrm{b}^k$
    Get the $\mathbf{Y}_\mathrm{proj}$ by (67) and solve (68) to get $\mathbf{Y}^k$
    Update the dual variables by (61), $k = k$+1
end
*After this loop, the solution for $\boldsymbol{X}_\mathrm{b}^\mathrm{bin}$ is obtained
Formulate the problem for the final result solution
while Eq (62) is met **do**
    Solve (58) with $\boldsymbol{X}_\mathrm{b}^\mathrm{bin}$ fixed to get $\mathbf{X}_\mathrm{b}^k$
    Solve (59) with $\boldsymbol{X}_\mathrm{b}^\mathrm{bin}$ fixed to get $\mathbf{Y}^k$
    Update the dual variables by (61), $k = k$+1
end
*After this loop, the solution for $\boldsymbol{X}_\mathrm{b}^\mathrm{cont}$ is obtained

C. Convergence Analysis of F-ADMM

The proposed F-ADMM method addresses the physical system restoration problem through three phases, and its overall convergence relies on the convergence of each phase. In the initial-value solution phase, the binary variables are relaxed into continuous ones, which converts the problem into a convex optimization problem. In the final result solution phase, the binary variables are fixed, and the problem remains convex. Since both phases are solved with the ADMM algorithm under convexity, their convergence is guaranteed. In the topology-solution phase, the modified P-ADMM algorithm is employed, where a penalty term is added to the original P-ADMM algorithm. Given that the topology solution problem exhibits the property of becoming convex upon relaxation of binary

variables, the P-ADMM algorithm is applicable for addressing this type of problem with convergence guaranteed [34]. Therefore, the convergence of the F-ADMM method for solving PSR model can be guaranteed.

The F-ADMM method presented above can be implemented on EC devices to solve the overall PSR model in a distributed manner. By fixing binary variables in advance, the number of iterations required is reduced, rendering it well-suited for EC devices with limited network lifetimes.

V. Case Study

To validate the effectiveness of the proposed method, two case studies are conducted in this paper. Several components of both the cyber system and physical system are assumed damaged after an extreme event, and the remaining EC devices are utilized to organize the distributed energy resources and restore the power supply. Parameters of the cyber system in the two cases are given in [35]. The max allowable hop count is set to 3. All DGs are assumed to operate in grid-following mode, with controllable active and reactive power outputs. Therefore, a bus block can only be restored when connected to the external grid, which provides the necessary voltage and frequency support as the main source. The restoration problem is solved using the YALMIP optimization toolbox with MATLAB R2022b and Gurobi 11.0 on a computer with an Intel Core i7-13700H CPU running at 2.10 GHz and 16 GB of RAM [36].

To evaluate the effectiveness of the proposed method, four methods are compared, including:

Method I: The physical system restoration is performed without preceding cyber system reconfiguration.

Method II: The cyber system is reconfigured by reassigning terminal devices from a faulty EC device to the nearest functioning EC device. Subsequently, physical network restoration is performed.

Method III: The cyber system is reconfigured by the distance-based k-means clustering method [38]. Subsequently, the physical network restoration is performed.

Method IV: CPS interdependent restoration is performed using the proposed method.

Method I represents the conventional centralized approach under extreme fault conditions, where most terminal resources cannot be controlled by the dispatch center and thus cannot participate in power restoration due to communication failures. Methods II and III illustrate two other types of cyber system restoration strategies that do not account for cyber-physical interdependency. Method IV is the proposed method.

Case A: IEEE 123-Node Test System

The IEEE 123-node test system, configured in a three-phase balanced manner [37], is used to evaluate the advantages of the proposed method in balancing the burdens of each EC device and reducing the number of uncontrolled terminal devices. Before the fault, 7 EC devices control the terminal devices, with loads supplied by the external grid near node 149. Faults are assumed to occur on the line between node 149 and the external grid, and simultaneously interrupt two EC devices.

The proposed method is used to restore power in the network, with the final result shown in Fig. 5. The lower-layer cyber system comprises 5 zones, each controlled by one EC device, while dashed lines in the upper layer indicate multi-hop links. In the physical system, the external power grid near node 300 supplies the network loads.

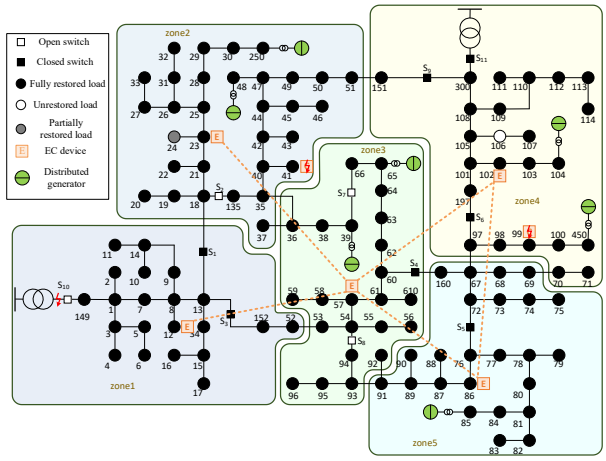

Fig.5. The final state of the IEEE 123-node test system.

(1) Comparison of cyber system restoration methods

The computational and communication burden of each EC device in methods I-IV is shown in Fig.6 and Fig.7. These burdens are constrained by the limited capacities of EC devices. If the burdens exceed these limits, the EC device will relinquish control of some terminal devices based on their distance. The terminal devices that are not controlled by any EC device are considered offline and cannot participate in physical network restoration. The effectiveness of cyber system restoration is evaluated by the number of uncontrolled terminal devices and the restored load value amount finally achieved in the physical system, as shown in TABLE I. The final restoration results with methods I-III are shown in Fig.8.

TABLE I
Comparison of Cyber System Restoration Result for Case A

Method	Uncontrolled terminal devices	Load value loss percentage %
Method I	36	91.70%
Method II	12	14.85%
Method III	15	29.85%
Method IV	0	0.04%

It is demonstrated that the proposed method results in the fewest uncontrolled devices and achieves the best restoration effect. As a comparison, in Method I, 36 terminal devices lose control and cannot participate in physical system restoration due to the faults of EC devices, resulting in 91.70% load value loss. In Methods II-III, the cyber system restoration methods fail to allocate terminal devices to the EC devices in a balanced manner. This results in some EC devices becoming overloaded, while others are not fully utilized. Consequently, EC devices are compelled to relinquish control of some terminal devices, resulting in some terminal devices being left uncontrolled. In Method II, the communication burdens in zone 2 and zone 3 exceed the limit. In Method III, the computational burdens in zone 2 and zone 5 exceed the limit.

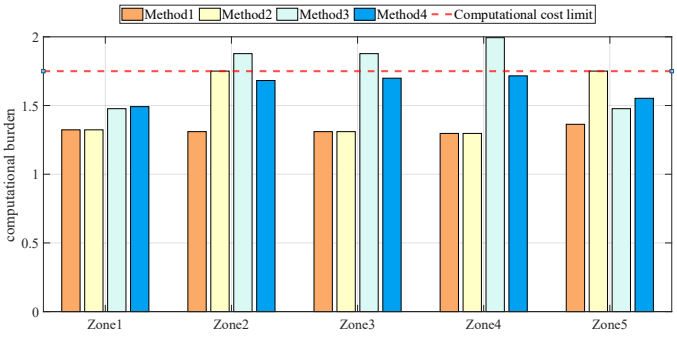

Fig.6. Computational burden of different methods in case A.

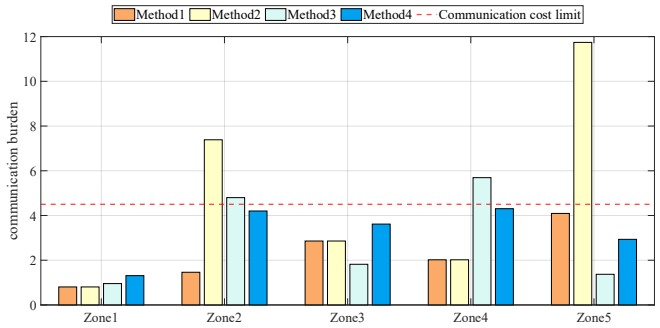

Fig.7. Communication burden of different methods in case A

To verify the impact of parameters ρ and r_c on the solution quality and speed of the cyber system restoration, a sensitivity analysis is conducted. The iterations number, decision-making rounds and average computational burden $\overline{O_i^{\mathrm{cp}}}$ of all EC devices are shown in Table III. It can be observed that, as ρ and r_c increase, the strategy generation is accelerated, but the average computational burden also rises. Excessive values of ρ and r_c can lead to a degradation in solution quality.

TABLE III
SENSITIVITY ANALYSIS OF PARAMETERS ρ AND r_c

	Parameter value	0.05	0.1	0.2	0.5
ρ	$\overline{O_i^{\mathrm{cp}}}$	1.63	1.63	1.63	1.66
	Iteration number	21	11	6	4
r_c	$\overline{O_i^{\mathrm{cp}}}$	1.63	1.63	1.66	1.69
	Decision-making round	75	58	51	32

The variance in computational burden versus iterations for different ρ values is depicted in Fig. 9. The variance oscillates and decreases with increasing iterations, and eventually falls below the allowable range, demonstrating the effectiveness of the proposed method.

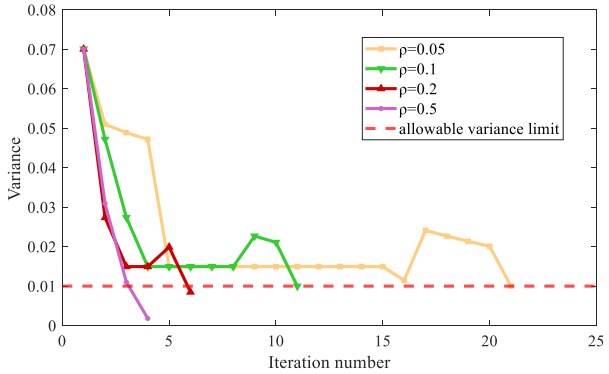

Fig.9. The variance in computational burden versus iterations with different ρ in case A.

Further studies are conducted to validate the effectiveness of the upper-layer restoration method under packet loss scenarios. In Case A, it is assumed that the packet loss rate of the communication link between EC devices 1 and 2 is high due to obstruction from buildings, while other links exhibit low packet loss rates. In this scenario, the proposed method is compared with two other network generation approaches, denoted as:

Method V: Only single-hop links are allowed to construct the upper-layer network.

Method VI: Multi-hop paths within the allowed hop count are enumerated, and the optimal one is selected.

TABLE IV presents the maximum number of paths requiring evaluation per EC device, the maximum power consumption across all EC devices, and the highest packet loss rate observed among all paths. In comparison to Method V, the multi-hop networks can reduce power consumption, thereby extending the network's survival time. Compared to Method VI, the proposed method significantly reduces the number of solutions that require evaluation, thereby improving efficiency.

TABLE IV
COMPARISON OF UPPER-LAYER CSR METHOD FOR CASE A

Method	Max number of paths evaluated	Max power consumption (W)	Max packet loss rate (%)
Method IV	12	5.99	5.92%
Method V	4	9.16	30.00%
Method VI	40	5.99	5.92%

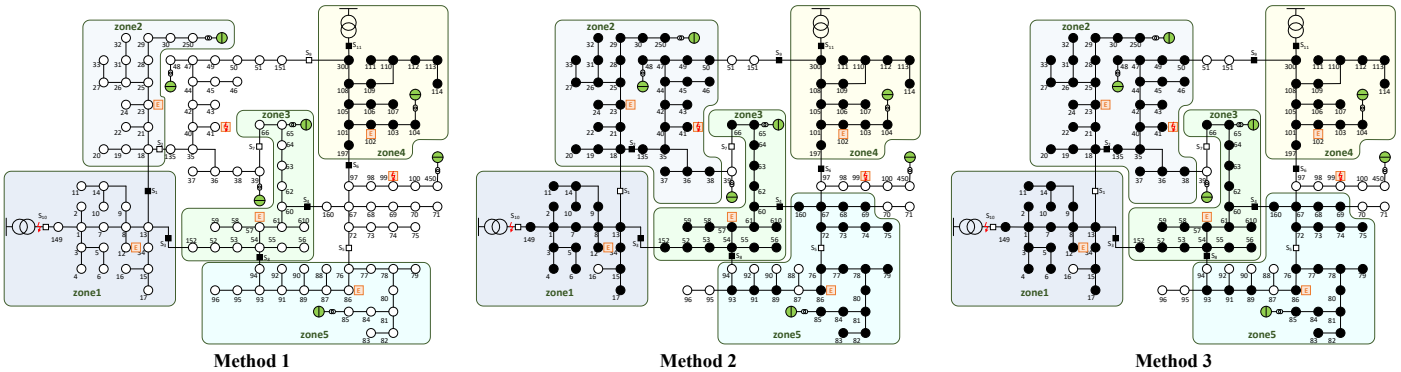

Method 1 **Method 2** **Method 3**

Fig.8. The final restoration results with different methods in case A

(2) Comparison of physical system restoration methods

To verify the effectiveness of the F-ADMM solving method, a comparison with the conventional ADMM method is conducted. Both F-ADMM and ADMM are applied to solve the PSR model based on the cyber system configuration obtained by Method IV. The results are presented in TABLE V. It should be noted that the computational time is theoretical because the process of distributed computation is simulated using a single computer by serially solving the problems that need to be solved by each EC device.

As shown in TABLE V, the proposed F-ADMM method significantly reduces computation time, which is important given the limited lifespan of emergency communication networks after a power failure. This improvement stems from the early fixation of binary variables, which are difficult to converge in the conventional ADMM method. The results demonstrate the method's feasibility and scalability in distribution networks with a large number of nodes.

TABLE V
COMPARISON OF F-ADMM AND ADMM METHODS FOR CASE A

Method	Iteration number	Computation time (s)
F-ADMM	60	7.09
ADMM	138	16.56

Case B. Taiwan 94-Node Test System

The Taiwan 94-node test system models a flexible distribution network with multiple interconnect switches. Under normal operation, 11 EC devices are deployed, each controlling a feeder, and two external grids supply the network. All tie switches are initially open. Faults are assumed to disrupt power on the left side, and simultaneously affect 5 EC devices. The remaining 6 EC devices coordinate the terminal devices, demonstrating the proposed method's efficacy under limited cyber-resource scenarios.

The final restoration result is shown in Fig. 10. In the lower-layer cyber system, the network is divided into 6 zones, each controlled by one EC device. Dashed lines in the upper layer indicate multi-hop links between EC devices. In the physical system, closing tie switches allows power from the right side to reach nodes on the left, while nodes outside EC control remain unpowered due to limited computation capability.

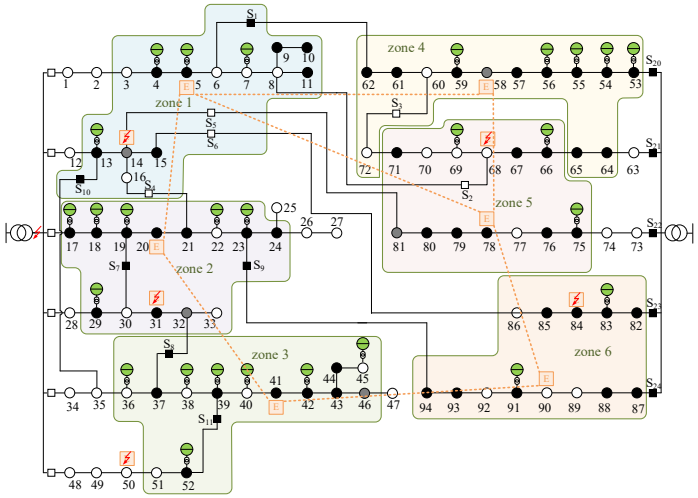

Fig.10. The final state of the Taiwan 94-node test system.

Due to the computational burden constraints of the EC devices, some terminal devices remain uncontrolled after the cyber system restoration. The number of uncontrolled terminal devices and the final restoration performance using different methods are shown in TABLE VI. As shown in TABLE VI, the proposed method has a better restoration effect than Methods I~III. This is because in other methods, the impact of cyber system restoration on the physical network restoration is not considered. Consequently, these methods do not prioritize control over critical terminal devices, resulting in a high proportion of critical devices among the uncontrolled devices, as depicted in Fig.11. This issue adversely affects the physical system restoration, leading to a worse restoration effect.

TABLE VI
COMPARISON OF CYBER SYSTEM RESTORATION RESULT FOR CASE B

Method	Uncontrolled terminal devices	Load value loss percentage %
Method I	31	41.08%
Method II	20	23.05%
Method III	21	24.00%
Method IV	16	17.39%

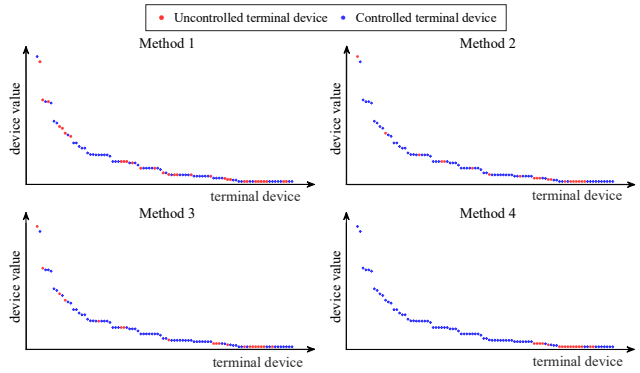

Fig.11. States of terminal devices of different methods in case B.

To verify the optimality of the proposed greedy-based cyber system restoration method, we compared it with the genetic algorithm (GA). While the GA focuses solely on minimizing the objective function (18), the proposed method also balances the computational burden across EC devices. Table VII reports the computation times. The proposed method shows a 6.7% deviation from the GA-based method, which is acceptable given its substantial reduction in solution time.

TABLE VII
COMPARISON OF THE PROPOSED METHOD AND GA FOR CASE B

Method	Result value of the objective function (18)	Solution time (s)
Proposed method	-18.89	0.19
GA-based method	-20.24	63.76

As shown in TABLE VIII, F-ADMM requires fewer iterations and less computation time than conventional ADMM. These results demonstrate the computational efficiency and scalability of the proposed method in complex networks with flexible structure and enhanced CPS interdependency.

TABLE VIII
COMPARISON OF F-ADMM AND ADMM METHODS FOR CASE B

Method	Iteration number	Computational time (s)
F-ADMM	53	6.36
ADMM	171	20.52

As shown in TABLE VIII, F-ADMM requires fewer iterations and less computation time than conventional ADMM. These results demonstrate the computational efficiency and scalability of the proposed method in complex networks with flexible structure and enhanced CPS interdependency.

To analyze the voltage errors introduced by the linearized Distflow model, the PSR models in MILP and MINLP formulations are compared. The MINLP model employs the standard Distflow constraint and can be considered the accurate result. Since the distributed method inherently introduces residuals between boundary variables, this paper utilizes centralized optimization solver to precisely compare the results of the two models. The result is shown in TABLE IX. The maximum deviation between the node voltages obtained from the two models is 0.06 p.u., which aligns with the analysis in Section II and demonstrates the feasibility of the linearized model.

TABLE IX
VOLTAGE OBTAINED USING MINLP AND MILP MODELS IN CASE B

Model	Highest voltage (p.u.)	Lowest voltage (p.u.)
MINLP model	1.05	1.00
MILP model	1.02	0.98

CONCLUSION

In this study, a CPS interdependent restoration method based on edge computing device is proposed, which considers the interaction of the cyber system and physical system during the restoration process. In cyber system restoration, EC devices establish emergency communication networks and organize the distributed terminal devices, supporting the optimization and implementation of the physical system restoration strategy. In physical system restoration, the F-ADMM method is proposed to generate power restoration strategy with fewer iterations, facilitating rapid power restoration in cyber systems with limited lifespan. The effectiveness of the proposed method is verified by two typical case studies, indicating the necessity and benefit of considering CPS interdependency in restoration.

The proposed method offers a cost-effective approach to enhance reliability by efficiently organizing medium- and low-voltage distributed resources, leveraging the networking and control capabilities of EC devices. Additionally, the method improves restoration efficiency and performance, particularly when both cyber and physical systems are compromised.

The limitations of the proposed method are mainly threefold. Firstly, this study considers only controllable grid-following DGs, where voltage and frequency are supported by the external grid. Future research to incorporate other types of DGs, such as grid-forming and uncontrollable renewable DGs, would be interesting. This would enable power restoration to be extended toward supporting islanded operation of zones under temporal variations. Secondly, this study mainly focuses on radial networks. Alternative operating structures, such as closed-loop networks, could be investigated in future research. Thirdly, the proposed method is lightweight to ensure its scalability in large-scale systems. However, as more EC devices participate in the restoration process, the decision-making time and convergence difficulty increase. This problem could potentially be mitigated by exploring network partitioning approaches to reduce the model scale.

REFERENCES

[1] Z. Li, Y. Xu, P. Wang, et al., "Restoration of a multi-energy distribution system with joint district network reconfiguration via distributed stochastic programming," *IEEE Trans. Smart Grid*, vol. 15, no. 3, pp. 2667-2680, May 2024.

[2] J. Zhao, Z. Zhang, H. Yu, et al., "Cloud-edge collaboration-based local voltage control for DGs with privacy preservation," *IEEE Trans. Ind. Inform*., vol. 19, no. 1, pp. 98–108, Jan. 2023.

[3] Z. Wei, K. Xie, B. Hu, et al., "Distribution system restoration with cyber failures based on co-dispatching of multiple recovery resources," in *J. Mod. Power Syst. Clean Energy*, vol. 12, no. 4, pp. 1096-1112, July 2024.

[4] Z. Liu, Q. Wu, X. Shen, et al, "Post-Disaster Robust Restoration Scheme for Distribution Network Considering Rerouting Process of Cyber System With 5G," IEEE Transactions on Smart Grid, vol. 15, no. 5, pp. 4478-4491, Sept. 2024.

[5] G. Liang, S. Weller, J. Zhao, et al, "The 2015 Ukraine Blackout: Implications for False Data Injection Attacks," IEEE Transactions on Power Systems, vol. 32, no. 4, pp. 3317-3318, July 2017.

[6] F. Shen, J. L´opez, Q. Wu, et al., "Distributed self-healing scheme for unbalanced electrical distribution systems based on alternating direction method of multipliers." *IEEE Trans. Power Syst*, May 2020, pp. 2190–99.

[7] W. Li, Y. Li, C. Chen, et al., "A full decentralized multi-agent service restoration for distribution network with DGs," *IEEE Trans. Smart Grid*, vol. 11, no. 2, pp. 1100–1111, Mar. 2020.

[8] S. Konar, A. K. Srivastava and A. Dubey, "Distributed optimization for autonomous restoration in DER-rich distribution system," *IEEE Trans. Power Delivery*, vol. 38, no. 5, pp. 3205-3217, Oct. 2023.

[9] B. Fan, X. Liu, G. Xiao, et al., "Attention-based multiagent graph reinforcement learning for service restoration," in *IEEE Trans. Artif. Intell.*, vol. 5, no. 5, pp. 2163-2178, May 2024.

[10] F. Shen, Q. Wu, J. Zhao, et al., "Distributed risk-limiting load restoration in unbalanced distribution systems with networked microgrids." *IEEE Trans. Smart Grid*, vol. 11, no. 6, Nov. 2020, pp. 4574–86.

[11] R. R. Nejad and W. Sun, "Enhancing active distribution systems resilience by fully distributed self-healing strategy." *IEEE Trans. Smart Grid*, Mar. 2022, pp. 1023–34.

[12] B. Chen, J. Wang, X. Lu, et al., "Networked microgrids for Grid resilience, robustness, and efficiency: a review," *IEEE Trans. Smart Grid*, vol. 12, no. 1, pp. 18-32, Jan. 2021.

[13] R. He, H. Liang, J. Wu, et al., "Reliability assessment of cyber-physical distribution system using multi-dimensional information network model," *IEEE Trans. Smart Grid*, vol. 14, no. 6, pp. 4683-4692, Nov. 2023.

[14] X. Liu, B. Zhang, B. Chen, et al., "Towards optimal and executable distribution grid restoration planning with a fine-grained power-communication interdependency model," *IEEE Trans. Smart Grid*, vol. 13, no. 3, pp. 1911-1922, May 2022.

[15] M. Tian, Z. Dong, L. Gong, et al., "Coordinated repair crew dispatch problem for cyber–physical distribution system," *IEEE Trans. Smart Grid*, vol. 14, no. 3, May 2023, pp. 2288–300.

[16] Z. Ye, C. Chen, R. Liu, et al., "Boost distribution system restoration with emergency communication vehicles considering cyber-physical interdependence," *IEEE Trans. Smart Grid*, vol. 14, no. 2, pp. 1262-1275, March 2023.

[17] H. Zhang, C. Chen, S. Lei, et al "Resilient distribution system restoration with communication recovery by drone small cells," *IEEE Trans. Smart Grid*, vol. 14, no. 2, pp. 1325-1328, March 2023.

[18] Y. Cao, Y. Luo, H. Yang and C. Luo, "UAV-based emergency communications: an iterative two-stage multiagent soft actor–critic approach for optimal association and dynamic deployment," I*EEE Internet Things J.*, vol. 11, no. 16, pp. 26610-26622, 15 Aug.15, 2024.

[19] Z. Liu, Q. Wu, X. Shen, et al., "Post-disaster robust restoration scheme for distribution network considering rerouting process of cyber system with 5G," *IEEE Trans. Smart Grid*, vol. 15, no. 5, pp. 4478-4491, Sept. 2024.

[20] P. -Y. Kong, "Routing in communication networks with interdependent power grid," *IEEE/ACM Trans. Netw.*, vol. 28, no. 4, pp. 1899-1911, Aug. 2020.

[21] C. Wang, M. Yan, K. Pang, et al., "Cyber-physical interdependent restoration scheduling for active distribution network via ad hoc wireless

communication," *IEEE Trans. Smart Grid*, vol. 14, no. 5, pp. 3413-3426, Sept. 2023.
[22] P. Ge, F. Teng, C. Konstantinou, et al., "A resilience-oriented centralised-to-decentralised framework for networked microgrids management," *Appl. Energy*, vol. 308, pp. 118234, Feb. 2022.
[23] S. Shang, X. Li, K. Gu, et al, "A robust privacy-preserving data aggregation scheme for edge-supported IIoT," *IEEE Transactions on Industrial Informatics*, vol. 20, no. 3, pp. 4305-4316, March 2024.
[24] H. Byeon, A. Mahmood, G. Sachin, et al, "Zero trust management over consumer technology-based IoT edge node for SDN communication and control of cyber–physical systems," *IEEE Transactions on Consumer Electronics*, vol. 71, no. 2, pp. 4849-4858, May 2025.
[25] Q. Sun and G. Yang, "Anti-disturbance secure state estimation for continuous-time cyber-physical systems under sparse sensor attacks," *IEEE Internet of Things Journal,* vol. 12, no. 16, pp. 34035-34043, 15 Aug, 2025.
[26] R. Rigo-Mariani, V. Vai. "An iterative linear Distflow for dynamic optimization in distributed generation planning studies," *International Journal of Electrical Power & Energy Systems,* 138, 107936, 2022.
[27] R. Jabr, R. Singh, and B. Pal, "Minimum loss network reconfiguration using mixed-integer convex programming," *IEEE Trans. Power Syst.*, vol. 27, no. 2, pp. 1106–1115, May 2012.
[28] Z. Liu, S. Olaf. "Efficient solution of distributed MIP in control of networked systems." *Proceedings in applied mathematics & mechanics*, vol. 20, no. 1, Jan. 2021.
[29] A. Termehchi and M. Rasti, "Joint sampling time and resource allocation for power efficiency in industrial cyber–physical systems," *IEEE Trans. Ind. Inform.*, vol. 17, no. 4, pp. 2600-2610, April 2021.
[30] IEEE Standard for Low-Rate Wireless Networks. IEEE Std 802.15.4-2015. Piscataway, NJ: IEEE, 2015.
[31] O. Badarneh, "The α-η-F and α-κ-F composite fading distributions," *IEEE Communications Letters,* vol. 24, no. 9, pp. 1924-1928, Sept. 2020.
[32] W. Xia, C. Di, H. Guo et al, "Reinforcement learning based stochastic shortest path finding in wireless sensor networks," *IEEE Access*, vol. 7, pp. 157807-157817, 2019.
[33] Y. Zheng and Q. Liu. "A review of distributed optimization: problems, models and algorithms." *Neurocomputing*, Apr. 2022, pp. 446–59.
[34] R. Takapoui, N. Moehle, S. Boyd, et al, "A simple effective heuristic for embedded mixed-integer quadratic programming," International Journal of Control, 93, 2-12, 2020.
[35] Detailed parameters of the case studies, 2025. [online]. Available: doi.org/10.6084/m9.figshare.28756667.v1
[36] J. Lofberg, "YALMIP: a toolbox for modeling and optimization in MATLAB," IEEE Xplore, Sep. 2004.
[37] C. Chen, J. Wang, F. Qiu et al, "Resilient distribution system by microgrids formation after natural disasters," IEEE Transactions on Smart Grid, vol. 7, no. 2, pp. 958-966, March 2016.
[38] S. Amit, P. Mukesh, G. Akshansh, et al. "A review of clustering techniques and developments." *Neurocomputing*, vol. 267, pp. 664–81, Dec. 2017.

Hao Yu (Senior Member, IEEE) received the B.S. and Ph.D. degrees in electrical engineering from Tianjin University, Tianjin, China, in 2010 and 2015, respectively.

He is currently an Associate Professor with the School of Electrical and Information Engineering, Tianjin University. His current research interests include the operation analysis and optimization of active distribution networks and integrated energy systems.

Dr. Yu serves as an Assistant Editor for both Sustainable Energy Technologies and Assessments and IET Energy Systems Integration.

Zhicheng Zhang received the B.E. degree in electrical engineering from Taiyuan University of Technology, Taiyuan, China, in 2023. He is currently working toward the master degree with Tianjin University, Tianjin, China, both in electrical engineering.

His research interests include power restoration for active distribution networks.

Peng Li (Senior Member, IEEE) received the B.S. and Ph.D. degrees in electrical engineering from Tianjin University, Tianjin, China, in 2014 and 2019, respectively.

He is currently a Professor with the School of Electrical and Information Engineering, Tianjin University. His current research interests include operation and planning of active distribution networks, modeling, and transient simulation of power systems.

Prof. Li is an Associate Editor of IEEE TRANSACTIONS ON SUSTAINABLE ENERGY, CSEE Journal of Power and Energy Systems, Sustainable Energy Technologies and Assessments, and IET Renewable Power Generation.

Haoran Ji (Senior Member, IEEE) received the B.S. and Ph.D. degrees in electrical engineering from Tianjin University, Tianjin, China, in 2014 and 2019, respectively.

He is currently a Professor with Tianjin University. His research interests include distributed generation systems and optimal operation of distribution networks.

Guanyu Song (Senior Member, IEEE) received the B.S. and Ph.D. degrees in electrical engineering from Tianjin University, Tianjin, China, in 2012 and 2017, respectively.

He is currently an Engineer with the School of Electrical and Information Engineering, Tianjin University. His current research interests include optimal planning and operation of smart distribution system.

Jiancheng Yu is currently with State Grid Tianjin Electric Power Company, Tianjin, China. His research interests include integrated energy, demand response, and smart power distribution and consumption.

Jinli Zhao (Member, IEEE) received the Ph.D. degree in electrical engineering from Tianjin University, Tianjin, China, in 2007.

She is currently an Associate Professor with the School of Electrical and Information Engineering, Tianjin University. Her research interests include operation and planning of active distribution networks and power system security and stability.

Jianzhong Wu (Fellow, IEEE) received the B.Sc., M.Sc., and Ph.D. degrees in electrical engineering from Tianjin University, China, in 1999, 2002, and 2004, respectively.

From 2004 to 2006, he was at Tianjin University, where he was an Associate Professor. From 2006 to 2008, he was a Research Fellow at the University of Manchester, Manchester, U.K. He is a Professor of Multi-Vector Energy Systems and the Head of the School of Engineering, Cardi University, Cardi , U.K. He is also the Co-Director of U.K. Energy Research Centre, London, U.K., and the EPSRC Supergen Energy Networks Hub. His research interests include integrated multienergy infrastructure and smart grid.

He is the Co-Editor-in-Chief of Applied Energy.